JOURNAL OF WATER AND LAND DEVELOPMENT
e-ISSN 2083-4535
Polish Academy of Sciences (PAN), Committee on Agronomic Sciences
Institute of Technology and Life Sciences (ITP)
JOURNAL OF WATER AND LAND DEVELOPMENT
2021, No. 49 (IV–VI): 35–46; https://doi.org/10.24425/jwld.2021.137094
Available (PDF): https://www.itp.edu.pl/JWLD; http://journals.pan.pl/jwld

Received 25.05.2020
Reviewed 24.07.2020
Accepted 16.09.2020

Assessment of groundwater vulnerability using the DRASTIC model: A case study of Quaternary catchment A21C, Limpopo River Basin, South Africa

Simeneh S. MOGES ✉, Megersa O. DINKA

University of Johannesburg, Faculty of Engineering and the Built Environment, Department of Civil Engineering Sciences, PO Box 524, Auckland Park, 2006 Johannesburg, South Africa

For citation: Moges S.S., Dinka M.O. 2021. Assessment of groundwater vulnerability using the DRASTIC model: A case study of Quaternary catchment A21C, Limpopo River Basin, South Africa. Journal of Water and Land Development. No. 49 (IV–VI) p. 35–46. DOI 10.24425/jwld.2021.137094.

Abstract

Groundwater is a vital resource for domestic, agricultural, industrial activities and ecosystem services. Despite its multiple purposes, the resource is under significant threat owing to increasing contamination from anthropogenic activities and climate change. Hence, in order to ensure the reliability and sustainable use of groundwater for the present and future generations, effective management of groundwater (quality and quantity) is highly important. This can be achieved by identifying areas more vulnerable to contamination and implementing protective measures. The present study aims at assessing the vulnerability of groundwater using GIS-based DRASTIC index in the Quaternary catchment (A21C) within Limpopo River Basin. The vulnerability index varied from 87 to 207. About 53.6% (408 km^2) of the catchment area also exhibited high risk of groundwater contamination mostly in central, north-eastern and western part of the sub-catchment. The medium and low vulnerability classes cover only 18.1% (137.5 km^2) and 21.7% (165.1 km^2) of the study area, respectively. The shallow groundwater at the Doornfontein Campus belongs to very high vulnerability area. The sensitivity analysis indicates that depth to water level, recharge, aquifer media, soil and topography are the important contributors to vulnerability assessment. The correlation analysis performed to validate the final vulnerability map shows a moderate positive correlation, indicating the model's applicability to the urbanised environment. The study indicates an area that is highly vulnerable to pollution, and hence protective measures are necessary for sustainable management of the groundwater resource in the study area. The result of this study can also be further improved and verified by using other vulnerability assessment models.

Key words: *A21C Quaternary catchment, DRASTIC model, groundwater vulnerability, sensitivity analysis, South Africa*

INTRODUCTION

Groundwater (GW) is a vital resource for domestic consumption, agricultural and industrial activities, and ecosystem services [CHEN *et al.* 2018; HOWARD 2014]. This resource is precious particularly in arid and semi-arid areas because these areas typically lack sufficient surface water resources due to either aridity of the climate and/or surface water pollution. Traditionally, GW has been considered as more resilient to pollution compared with surface water sources and it is rarely influenced to a greater extent by drought and climate change [HOWARD 2014]. However, contaminants from unregulated industries, urbanisation and agricultural activities are threatening GW availability and sustainability [DEVIC *et al.* 2014; KADAOUI *et al.* 2019; MACHIWAL *et al.* 2018a].

GW contamination is a hidden surface-subsurface process since it is not directly invisible from the surface. It can be noticed only once a spring or a well becomes contaminated, or the contaminant is released into surface waters [JANG *et al.* 2017]. Thus, it may take several years to notice and accurately assess GW contamination [JANG *et al.* 2017]. Once GW is polluted, its cleaning is expensive and time consuming. Additionally, data constraints, variation in geographical locations and physical inaccessibility impede monitoring of all waters and make remedial actions costly and often not practical in many areas [BABIKER *et al.* 2005; SHRESTHA *et al.* 2017]. The proverb "prevention is better than cure" is, therefore, crucial in the proper management of GW resource [BUTLER *et al.* 2010] because prevention is cheaper and easier than any remedial measures.

GW can be protected from pollution by the early identification of areas more vulnerable to contamination and the implementation of protective measures. To identify more susceptible areas, various methods have been developed by a number of researchers. These broadly include statistical methods, subjective methods or the overlay-index (GIS-based qualitative) and the physical process-based methods (quantitative approaches) [MACHIWAL *et al.* 2018b; National Research Council 1993]. The first two approaches focus on evaluating intrinsic vulnerability, while process-based models are designed to assess specific vulnerability [MACHIWAL *et al.* 2018b]. Intrinsic vulnerability is the vulnerability based on natural aquifer properties only, such as hydrological, geological and hydrogeological characteristics, whereas specific vulnerability is related to a specific contaminant or a group of contaminants and their relationship with various features of the intrinsic vulnerability [HASAN *et al.* 2019; National Research Council 1993; OKE, FOURIE 2017].

The application of each method depends on the availability of sufficient quantitative and qualitative data and their spatial distribution, purpose and scale of mapping, costs associated with the formulation of the model and the specific hydrogeological settings of the aquifer being studied [AYDI 2018; RIBEIRO *et al.* 2017]. Overlay-index techniques are extensively used in the groundwater vulnerability assessment and more frequently appear in many scholarly publications. Of these, the DRASTIC model (depth to water level (D), net recharge (R), aquifer media (A), soil media (S), topography (T), impact of the vadose zone (I), and the hydraulic conductivity (C)) is one of the most popular methods of groundwater vulnerability (*GWV*) mapping and has been used in several countries, such as in the USA [JANG *et al.* 2017], Algeria [BOUFEKANE, SAIGHI 2018], DR Congo [KIHUMBA *et al.* 2017], Ecuador [RIBEIRO *et al.* 2017], Pakistan [MUHAMMAD *et al.* 2015], Malaysia [NESHAT *et al.* 2014], India [GUPTA 2014], Namibia [HAMUTOKO *et al.* 2016], and South Africa [LYNCH *et al.* 1994; 1997]. The broad application of the DRASTIC model in many areas is mainly due to the method's simplicity to use, low application cost; requirements of limited input data, less computational needs because it does not require a complex numerical analysis or a simulation process that involves many parameters, and produces an end product that is easily interpretable and incorporated into the decision-making process [ALLER *et al.* 1987; JANG *et al.* 2017].

Previously, some vulnerability assessments were conducted at the national and local levels (site-specific scale) in South Africa. These include an assessment conducted to develop a groundwater vulnerability map of South Africa by LYNCH *et al.* [1994; 1997], SAAYMAN *et al.* [2007], and MUSEKIWA and MAJOLA [2013], and local studies by MALHERBE *et al.* [2018], and SAKALA *et al.* [2018]. These studies help to identify the most vulnerable areas and inform decision-makers to implement groundwater pollution protection measures. However, the works were done on coarse spatial scale. The regional groundwater vulnerability assessment may not provide much accurate information at the catchment level. Furthermore, there is no separate groundwater vulnerability study conducted explicitly in the current study area (A21C Quaternary catchment). The objective of this study is to assess the vulnerability of GW of A21C Quaternary catchment using GIS-based DRASTIC method. The specific objectives are (i) to determine the vulnerability of shallow groundwater of Doornfontein Campus (DFC) relative to A21C sub-catchment; (ii) to determine the sensitivity of DRASTIC parameters, and (iii) to validate the vulnerability assessment using nitrate.

STUDY AREA

The A21C Quaternary catchment is situated between 25°52'23.69" S and 26°11'54.81" S and, 27°54'14.23" E to 28°12'24.69" E, whereas the shallow groundwater of the DFC Campus, University of Johannesburg, is located between 26°11'43.89" S and 28°03'21.15" E under the basements of Perskor Building, Gauteng Province, South Africa (Fig. 1). Hydrologically, it is located within the upper Crocodile River Catchment and regionally within Limpopo River Basin. The multiyear average precipitation is about 690 mm per annum, mostly concentrated in summer months. The summer rainfall significantly contributes to groundwater recharge [ABIYE *et al.* 2011]. The dry rainfall period corresponds to the lowest average temperatures, where July has the lowest recorded temperature values. The summer rainfall period corresponds to warmer temperature with February being the hottest. Higher and lower evaporation occurs in summer and winter seasons, respectively. The sub-catchment has a total area of about 760.6 km^2 and mainly characterised by urban setting where built ups occupy about 67% of the sub-catchment. Grasslands, cultivated areas, and forests occupy 14%, 6.8% and 6.6% of the sub catchment, respectively and the rest are covered by miscellaneous such as water bodies, shrubs, mines and quarries, etc. The natural topography of the study area is characterised by a moderate sloping elevation gradually decreasing from south to north and drained by the Jukskei River that starts around Doornfontein area in the south and flows to north direction.

Crystalline basement rocks are the dominant geological formations in the sub-catchment followed by Witwatersrand, Ventersdorp super groups respectively. The crystalline basement rocks are the oldest rock types in the sequence and consist of greenstone remnants, basement gneissic, granitic and migmatite rock types that are weathered and fractured at shallow depth and massive at deeper levels [ABIYE 2011; MCCARTHY, RUBIDGE 2005]. The Witwatersrand supergroup is further divided into the lower group, West Rand group, upper group, and the Central Rand group. The Central Rand group is represented by the Johannesburg and the Turffontein subgroups, which consist mostly of quartzites, conglomerate, and shale. The West Rand group is also characterised by three subgroups: Hospital Hill, Government and Jeppestown, which are characterised by quartzites, conglomerates, and shales [KOSITCIN *et al.* 2003]. Rocks of the Klipriversberg group and the Ventersdorp supergroup can also be found near the CBD and south of the city. These rocks are overlain by lava, both porphyrite and aphyric types. They are also overlaid by tuffs, shales, agglomerates and poorly sorted conglomerates [DE BEER 1986]. The Doornfontein Campus is mostly underlain by basaltic lava, agglomerate, and tuff from Klipriversberg subgroup and quartzites, conglomerates, and shales of the West Rand group.

In terms of geohydrology, the sub-catchment is predominated by the intergranular and fractured aquifers of genesis rocks that bear groundwater from 0.5–2 $dm^3 \cdot s^{-1}$. The groundwater is usually tapped from the shallow weathered rocks, and fractured zones of lower depth solid. The average borehole depth in the sub-catchment is about 15.2 m where water table elevation is decreasing from the upland area in the south to low lying areas in the north-west. Groundwater flows from higher elevation areas in the south to north-west. According to the DWS [2019] national integrated water information system, the available, recharge, reserve and abstracted amount of groundwater/year is estimated respectively at $1.07 \cdot 10^6$, $18.6 \cdot 10^6$, $1.95 \cdot 10^6$ and $2.17 \cdot 10^6$ $m^3 \cdot y^{-1}$. Moreover, the sub-catchment has an estimated surplus amount of groundwater of $14.56 \cdot 10^6$ $m^3 \cdot y^{-1}$. The location of the study area and geological formations are shown in Figures 1 and 2.

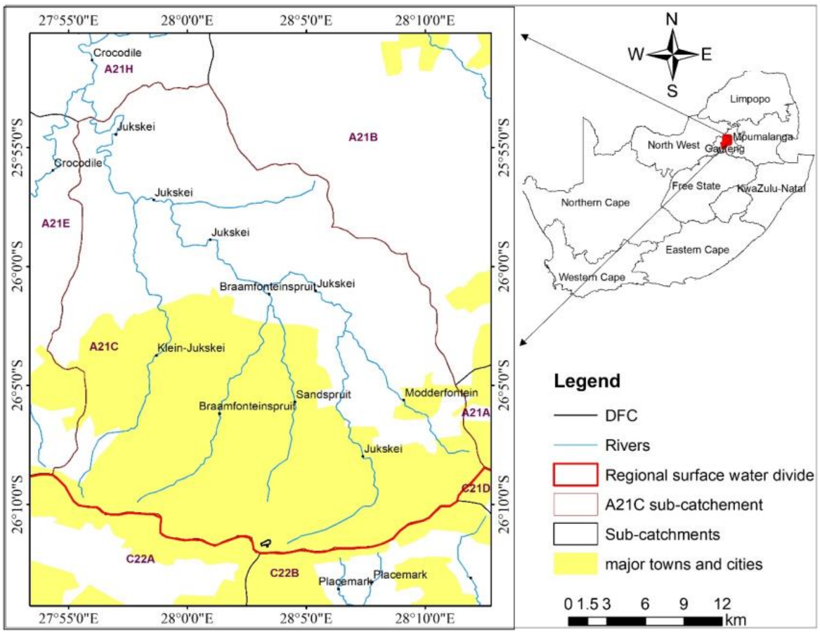

Fig. 1. Location of the study area; source: own elaboration

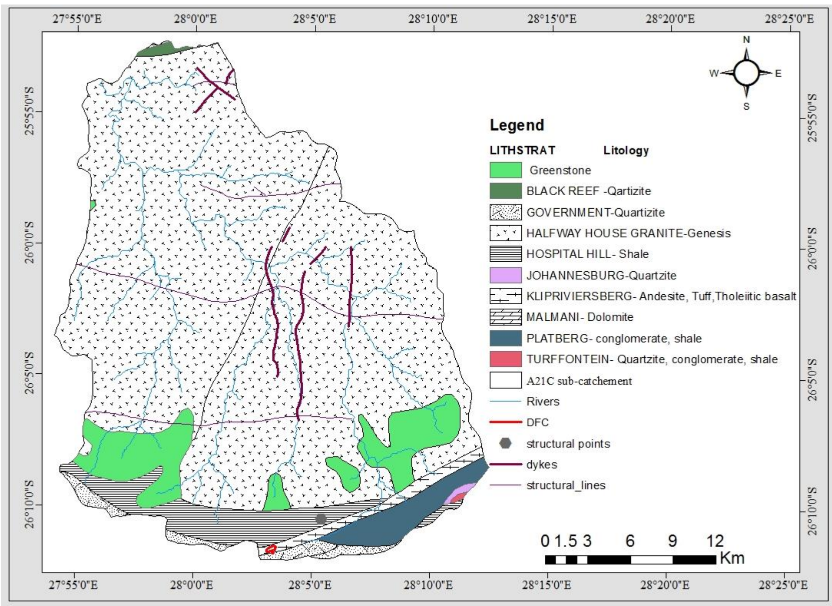

Fig. 2. Simplified A21C sub-catchment modified from the Council for Geoscience [2019]

MATERIALS AND METHODS

VULNERABILITY ASSESSMENT

The groundwater vulnerability was assessed using the GIS linked DRASTIC model. DRASTIC is a standardised model developed in the USA by ALLER *et al.* [1987] for evaluating the pollution potential of a specific area using known hydrogeological properties. It has three essential features: hydrogeological parameters, rating system and parameter weights. The seven hydrogeological parameters are those that contribute to its name DRASTIC: depth to water level (*D*), net recharge (*R*), aquifer media (*A*), soil media (*S*), topography (T), impact of the vadose zone (*I*), and the hydraulic conductivity (*C*) [ALLER *et al.* 1987; RIBEIRO *et al.* 2017]. Each of these hydrogeological variables were assigned a rating of 1 to 10 based on a range of values in which 1 denotes least vulnerable and 10 the most vulnerable areas. The hydrogeological parameters are further assigned to relative weights from 1 to 5, where the most significant parameters have the weight of 5 while the least significant the weight of 1 [KIHUMBA *et al.* 2017]. Ratings and weights of each parameter are then multiplied and added to provide vulnerability index values by applying the following linear equation [ALLER *et al.* 1987]:

$$DR_i = D_w D_r + R_w R_r + A_r A_w + S_r S_w + T_r T_w + I_w I_r + C_w C_r \tag{1}$$

where: DR_i = DRASTIC vulnerability index, *D*, *R*, *A*, *S*, *T*, *I*, and *C* represents the seven parameters of the model; *w* = assigned weight of DRASTIC parameter; *r* = assigned rate for the respective DRASTIC parameter.

INPUT DATA PREPARATION AND PROCESSING

Various input data used for the vulnerability assessment and their sources are shown in Table 1. These data were processed in the same workspace in ArcGIS 10.5.1 and projected properly using projection coordinate of WGS_1984_UTM_Zone_35S. The data were then reclassified and ranked to produce individual DRASTIC parameter layers.

Table 1. Data type, and source for preparing DRASTIC parameter layers

Data type	Data source	Format	Output layer
Borehole water level (m)	DWS National Groundwater Archive	CSV table	*D*-raster
Net recharge ($mm \cdot y^{-1}$)	Water Resources of South Africa 2012 Study [WR 2012]	raster	*R*-raster
Soil	Water Resources of South Africa 2012 Study [WR 2012]	vector	*S*-raster
Geological map	South Africa Council for Geoscience	vector	*A*-raster
Digital elevation model (DEM)	The 30-meter STRM data from USGS	raster	*T*-raster
Hydrogeological maps	DWS 1:500,000 hydrogeological map [BARNARD 1999]	vector	*I*-raster
Hydraulic conductivity ($cm \cdot d^{-1}$)	literature [DOMENICO, SCHWARTZ 1998; YOUNGER 2009]	pdf	*C*-raster
Nitrate	measurement and DWS National Groundwater Archive	CSV table	NO_3 – vector

Source: own elaboration.

RATING AND WEIGHTING OF DRASTIC PARAMETERS

The rates and weights assigned for DRASTIC parameters are shown in Tables 2 and 3. Rating and weighting systems were developed according to guidelines prepared by ALLER *et al.* [1987] and for South Africa by LYNCH *et al.* [1994]. Rating values range from 1 to 10, where higher values are given for more significant parameters contributing to pollution.

Table 2. The rating of DRASTIC parameters in the study area

Parameter	Measurement unit	Range	Rate
Depth to water level (*D*)	m	0–5	10
		5–15	7
		15–30	3
		>30	1
Net recharge (*R*)	$mm \cdot y^{-1}$	10–50	6
		50–100	8
Aquifer media (*A*)	–	dolomite	10
		intergranular and fractured	8
		fractured	6
Soil media (*S*)	–	sandy loam	6
		sandy clay loam and loam	5
Topography (*T*)	%	0–2	10
		…	.
		>18	1
Impact of vadose zone (*I*)	–	Witwatersrand	6
		Ventersdorp	4
		Genesis	3
		Transvaal	9
Hydraulic conductivity (*C*)	$m \cdot day^{-1}$	from 10^3 to 10^2	9
		…	…
		from 10^{-4} to 10^{-1}	6

Source: own elaboration.

Table 3. Weights of DRASTIC parameters

Parameter	Weight	Parameter	Weight
Depth to water level (*D*)	5	Topography (*T*)	1
Net recharge (*R*)	4	Impact of vadose zone (*I*)	5
Aquifer media (*A*)	3	Hydraulic conductivity (*C*)	3
Soil media (*S*)	2		

Source: own elaboration.

DEVELOPMENT OF VULNERABILITY INDEX MAPS

Final vulnerability index maps were developed by overlapping each of the rated individual thematic maps showing DRASTIC parameters with their respective weighting values and summing up their results using Equations (1) and (2). The multiplication and summation of parameters were undertaken by using the raster calculator within the Arc GIS map algebra tool. Vulnerability indices were calculated on a grid map with a cell size of 20 m × 20 m. Results were classified into different classes using natural breaks (Jenks)

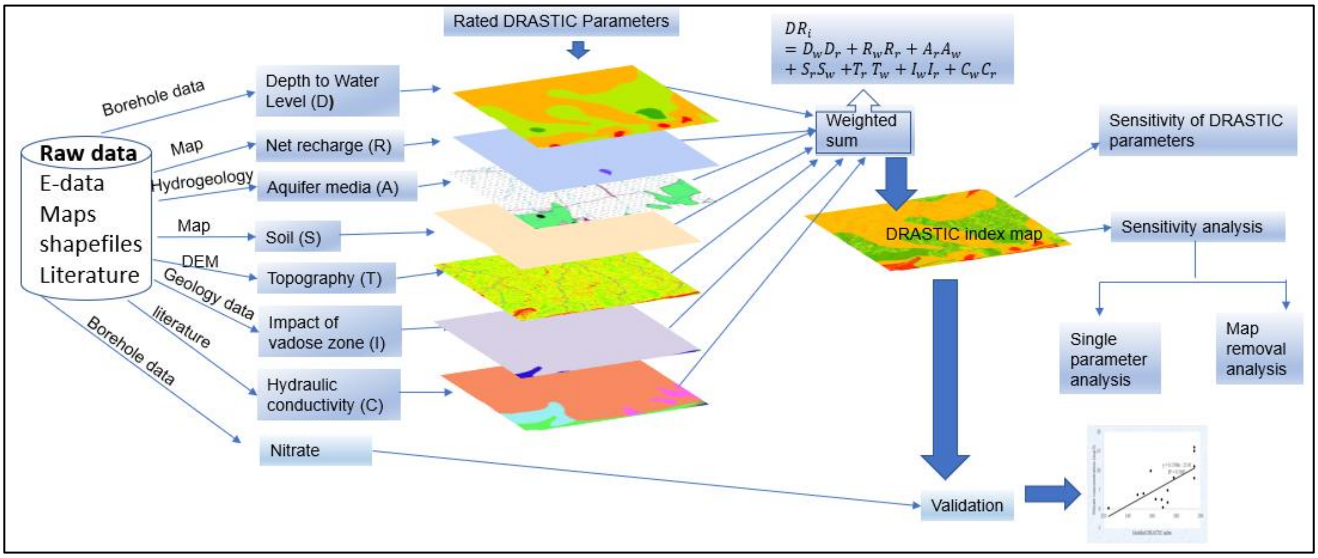

Fig. 3. Flow chart showing methodology adapted to produce vulnerability index maps: source: own elaboration

classification techniques. The overall theoretical framework scheme followed to produce vulnerability index maps as indicated in Figure 3.

SENSITIVITY ANALYSIS

In order to identify how the change in an input parameter affects other parameters and overall vulnerability assessment results, sensitivity analyses were performed in many studies [AKBAR, AKBAR 2013; SAIDI *et al.* 2011; VU *et al.* 2019]. The sensitivity analysis plays a vital role in minimising errors and selecting dominant parameters during a vulnerability assessment. The two commonly applied sensitivity analyses in groundwater vulnerability assessment using the DRASTIC model are the single parameter sensitivity analysis (SPSA) [NAPOLITANO *et al.* 1996] and map removal sensitivity analysis (MRSA) [LODWICK *et al.* 1990].

The single parameter sensitivity. The single parameter sensitivity analysis (SPSA) method examines the effective weight of DRASTIC parameters with respect to rates and theoretically assigned weights to the variables [NAPOLITANO *et al.* 1996]. The parameter's effective weight is calculated by applying Equation (2) [KUMAR, PRAMOD KRISHNA 2019; NAPOLITANO *et al.* 1996]:

$$W = \frac{P_r\,P_w}{V}100 \tag{2}$$

where: W = the "effective" weight of each parameter; P_r and P_w = rating and weight of each variable, respectively; V = the overall vulnerability index.

Map removal sensitivity analysis. The map removal sensitivity analysis (MRSA) is the study of how the sensitivity of the DRASTIC map changes when one or more parameters are removed from the vulnerability analysis [LODWICK *et al.* 1990; SAIDI *et al.* 2011]. The MRSA is executed by eliminating a parameter from the model and then evaluating influence on DRASTIC model results [KUMAR, PRAMOD KRISHNA 2019]. The purpose of the MRSA analysis is mainly to determine those parameters whose exemption from the analysis does not significantly influence the accuracy of results. The MRSA index is calculated by using Equation (3) [LODWICK *et al.* 1990]:

$$S = \left|\frac{\frac{V}{N}-\frac{V'}{n}}{V}\right|100 \tag{3}$$

where: S = the sensitivity expressed as variation index, V and V' = the vulnerability indices of unperturbed and perturbed outputs, respectively, and N and n = the numbers of data layers used for calculating V and V', respectively.

When all DRASTIC variables are used during sensitivity analysis, it is referred to as an unperturbed vulnerability, whereas if a few parameters are considered, then it is known as a perturbed vulnerability [KUMAR, PRAMOD KRISHNA 2019].

VALIDATION OF VULNERABILITY MAPS

Validation is an integral part of modelling and helps to produce reliable and accurate results. In groundwater vulnerability assessment, NO_3^- is commonly used as a validation parameter due to its non-lithological/very low presence in groundwater under natural conditions [HASAN *et al.* 2019]. The presence of NO_3^- in groundwater could reveal pollutant sources such as from urban waste, agricultural activities. Several studies such as SINGH *et al.* [2015], KOZŁOWSKI and SOJKA [2019], HASAN *et al.* [2019], KUMAR and PRAMOD KRISHNA [2019] and VU *et al.* [2019] have used NO_3^- as an effective validation parameter for vulnerability assessment model results. In this study, nitrate concentrations measured and obtained from the national groundwater archive within the study area were used to validate the final vulnerability map. The NO_3^- values map was created and superimposed on the vulnerability index map. Index values for the respective NO_3^- concentrations in boreholes were then extracted using ArcGIS and Extract Values to Points, and plotted to observe the correlation between the two.

RESULTS AND DISCUSSION

CHARACTERISATION OF DRASTIC PARAMETERS

The individual DRASTIC GIS maps were created based on each set criteria, indicating the relative groundwater vulnerability. These are displayed below in the order of DRASTIC. Each of parameters is also discussed in the subsequent sub-sections.

Depth to water level (*D*). Higher values of *D* are located in the southern side of the catchment, whereas lower *D* values mostly belong to the northern side of the A21C catchment mimicking the surface topography (Fig. 4). According to the DRASTIC assumption, areas with low *D* values are more prone to pollution and rated with higher values, whereas those with higher *D* values are less susceptible to pollution and rated with low values. The *D* values were assigned ratings that range from 1 (the lowest) to 10 (the highest) and a weight of 5 based on and LYNCH *et al.* [1994] as shown in Table 4.

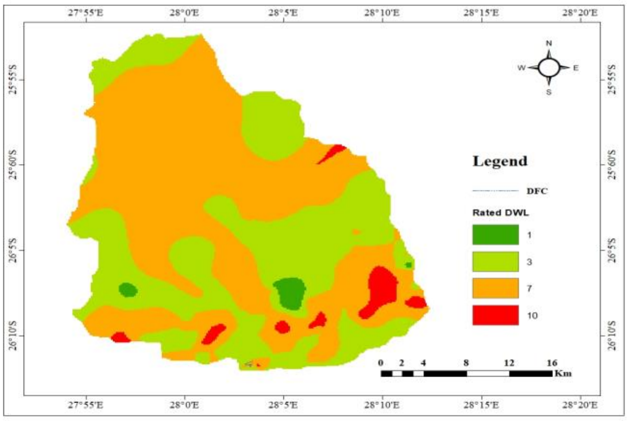

Fig. 4. Rated map of depth to water level (*D*); source: own study

Table 4. Depth to water level (*D*)

Depth range (m)	Rate	Area coverage (%)
0–5	10	2.7
5–15	7	56.9
15–30	3	39.2
>30	1	1.2

Source: own study.

Net recharge (*R*). Ratings and weights of the net recharge map are summarised in Figure 5, and Table 5. As Figure 5 shows, the entire catchment area is characterised by a recharge rate of below 50 mm·y^{-1}, which is commonly described as a lower net recharge area. Smaller portions of the catchment get the recharge of about 51 mm·y^{-1}. According to DWAF [2006], the mean recharge rates within the A21C sub-catchment is about 41 mm·y^{-1}. Recharge is the main sources for groundwater replenishment of natural and artificial origins. It is described as the volume of available water that infiltrates via the unsaturated zone and reaches the groundwater table [HUANG *et al.* 2017]. Recharge plays a critical role in leaching and transporting of contaminants from the ground surface to the aquifer [ALLER *et al.* 1987]. The quantity of recharge also affects the dilution and dispersal of pollutants in the unsaturated and saturated zones. As recharge to the aquifer is higher, the potential of groundwater to pollution is also higher (higher vulnerability) because higher recharge promotes the higher downward movement of contaminants.

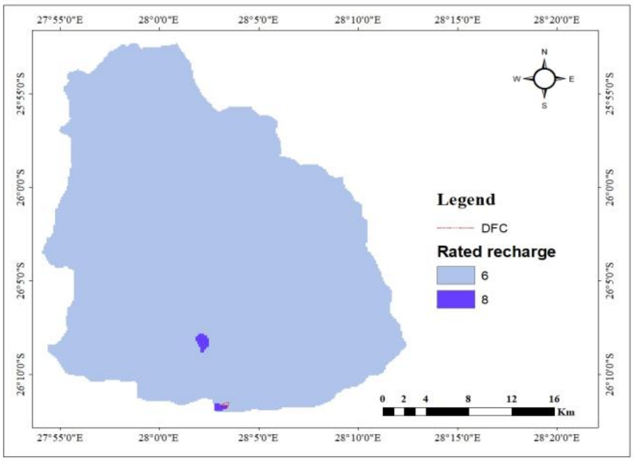

Fig. 5. Rated map of net recharge (*R*); source: own study

Table 5. Net recharge rate (*R*)

Range of net recharge (mm·y^{-1})	Rate	Area coverage (%)
10–50	6	99.73
50–100	8	0.25

Source: own study.

Aquifer media (*A*). Approximately 80% of the study area is covered with intergranular and fractured rocks that bear groundwater from 0.5–2 dm^3·s^{-1} and with a minor portion that yield 0.1–0.5 dm^3·s^{-1} (Fig. 6). A rating of 6 and 3 is assigned for these rocks. The southern part of the sub-catchment, which is mainly based on West rand and Klipriviersberg geological formation, has fractured aquifers with yields ranging from 0.5 to 2 dm^3·s^{-1}. A rating of 8 is assigned to this formation. A tiny portion in the north end of the sub-catchment belongs to the karstic aquifer which yields more than 5 dm^3·s^{-1}. This formation has been given a rating of 10 because of the presence of the karstic formation which most likely favours contaminant permeability

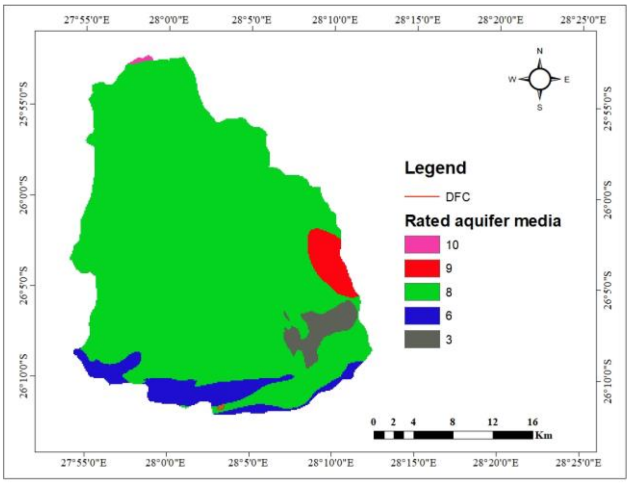

Fig. 6. Rated map of aquifer media (*A*); source: own study

[OUEDRAOGO *et al.* 2016]. A weighting of 4 is assigned to the aquifer media, according to ALLER *et al.* [1987] and LYNCH *et al.* [1994]. The rating of aquifer media is presented in Table 6. The aquifer media is a parameter that represents consolidated or unconsolidated geological formation that has abundant porous materials to yield adequate quantities of water to wells or springs [ALLER *et al.* 1987; HUANG *et al.* 2017]. The aquifer media affects the contaminant travel time and the natural process occurring during contaminant migration such as dispersion, sorption and reactivity [ALLER *et al.* 1987]. Aquifers with coarse or larger grain size formations (sandy, gravel) or highly fractured formations have higher permeability and lower travel time which leads to greater vulnerability.

Table 6. Rates and coverage of aquifer media

Range	Yield ($dm^3 \cdot s^{-1}$)	Rate	Area coverage (%)
Dolomite, karst	>5	10	0.14
Fractured	0.5–2.0	6	6.15
Intergranular and fractured	0.5–2.0	8	88.20
Intergranular and fractured	0.1–0.5	4	2.91
Intergranular and fractured	2.0–5.0	9	2.60

Source: own study.

Soil (S). Two types of soils are identified in the study area, namely sandy loam and sandy clay loam and loam (Fig. 7). Almost all (99%) of the sub-catchment is covered with sandy loam whereas only a small percentage (1.1%) of the area is covered with sandy clay loam (Tab. 7). The sandy loam texture of much of the sub-catchment promotes recharge as coarser textured soils have better permeability and infiltration. According to LYNCH *et al.* [1994], a rating has been assigned to soil texture classes. The higher rating 6 is assigned for sandy loam soils, and lower rating 5 is assigned for sandy clay loam (Tab. 7), whereas 2 is assigned to a weightage. The soil has an important impact on both water flow and contaminant transport because it acts as the most immediate recipient of rainfall and surface pollutants. The texture or the size of soil particles influences the rate at which water and contaminants percolate downward through

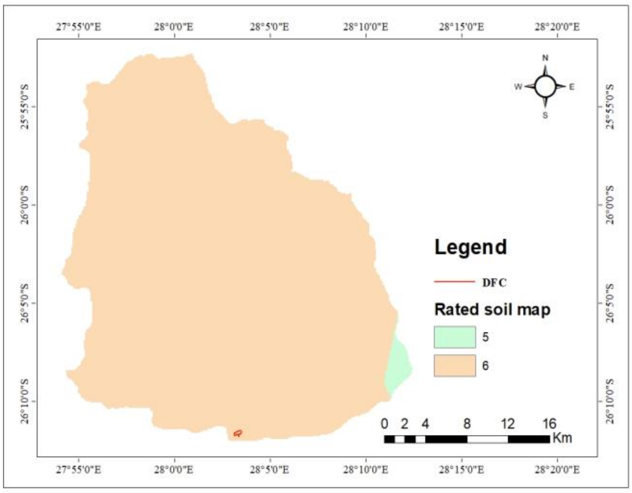

Fig. 7. Rated map of soil (*S*); source: own study

Table 7. Rates and coverage of soil media

Soil range	Rate	Area coverage (%)
Sandy loam	6	98.9
Sandy clay loam and loam	5	1.1

Source: own study.

the soil profile. Coarse textured soils (e.g. sandy or thin soils) permit contaminants to travel faster via open spaces allowing contaminants to reach water table easily whereas fine-textured soils such as clay and silt material have low permeability and hence restricts the downward movement of contaminant and have high attenuation process, resulting in less potential to contamination.

Topography (T). The rated *T* map is shown in Figure 8. The slope of the study area ranges from 0–18% and it is further divided into five classes based on ALLER *et al.* [1987] and LYNCH *et al.* [1994]. A tiny portion of the area has a very gentle inclination (0–2%). Since such areas are more prone to contamination, a rating of 10 is assigned to this class. The majority (35 and 47%) of the sub-catchment area has the inclination of 2–6% and 6–12%, respectively (Tab. 8). Both areas can be characterised with a moderately gentle slope (<12%) and hence there is also a higher possibility of contaminant infiltration. Ratings of 9 and 5 are assigned to inclinations of 2–6% and 6–12%, respectively. The remaining 10 and 2.6 % of the sub–catchment areas have inclinations of 12–18% and >18% respectively. Ratings of 3 and 1 are assigned for these areas due to their minimal possible impact on the vulnerability of groundwater. A weighting of 1 is assigned to the T based on ALLER *et al.* [1987] and LYNCH *et al.* [1994]. Topography plays a vital role in water movement and influences the rainfall–runoff and infiltration process in the area hydrogeological system.

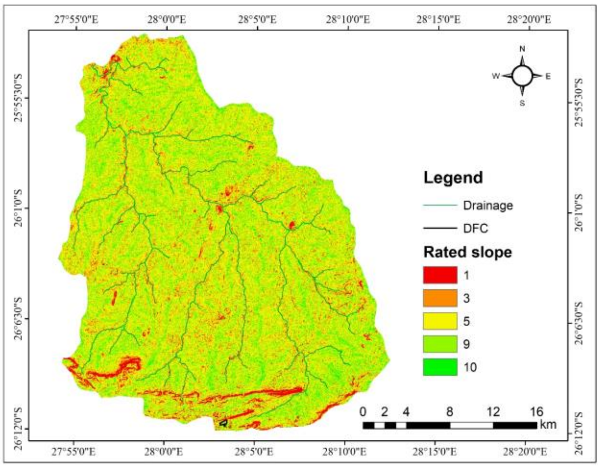

Fig. 8. Rated map of topography (*T*); source: own study

Table 8. Rates and coverage of topography (*T*)

Range of coverage of topography (%)	Rate	Area coverage (%)
0–2	10	5.3
2–6	9	35.3
6–12	5	47.0
12–18	3	9.9
>18	1	2.6

Source: own study.

The steeper topography is in an area, the greater the possibility of creating high surface runoff resulting in lower infiltration whereas, gentle slope topography area may have lower surface runoff and have the higher water holding capacity, i.e. greater the chance of high infiltration, favouring the groundwater to contamination.

Impact of the vadose zone (*I*). The rated *I*-map and its respective spatial coverage are presented in Figure 9 and Table 9, respectively. About 88.3, 7.17 and 4.23% of the study area is characterised by granite-genesis Witwatersrand, and Ventersdorp formations (Tab. 9). The *I* is known as the unsaturated section of the subsurface zone that contains pores filled by either air or water where physical and chemical processes take place, such as chemical reactions, dispersion, biodegradation, and volatilisation. The *I* is an essential variable in groundwater vulnerability assessment because it plays a vital buffering role between the aquifer and ground surface during water and contaminant infiltration [JAHAN *et al.* 2018]. The *I* formation is particularly important as it affects the contaminant percolation rate below the soil layer and above the groundwater table. Coarser grain size formation or intense fractured media have higher groundwater vulnerability because these types of formations permit contaminants to travel easily, whereas fine grain size formations or less fractured media have low groundwater vulnerability because of restrictions to water and contaminant flow. According to LYNCH *et al.* [1994], the dolomite formation was assigned the highest rating (10), whereas the lowest rating (3) were assigned to the granite-genesis formation. For quartzite, shale, and conglomerate of Witwatersrand, and andesite and tuff of the Ventersdrop formation, ratings of 6 and 4 were assigned. A weight of 4 is assigned to the *I* according to ALLER *et al.* [1987] and LYNCH *et al.* [1994].

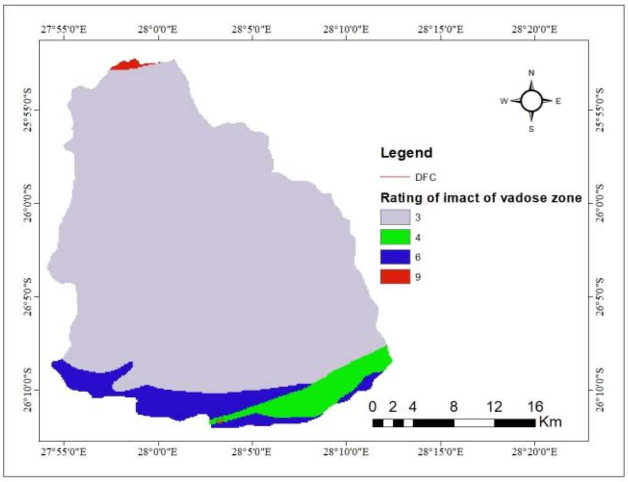

Fig. 9. Rated map of the impact of the vadose zone (*I*); source: own study

Table 9. Rates and coverage of the impact of the vadose zone (*I*)

Range of the impact of the vadose zone	Lithology	Rate	Area coverage (%)
Witwatersrand	quartzite, shale, conglomerate	6	7.17
Ventersdorp	tholeiitic basalt andesite, tuff	4	4.23
Genesis	granite-gneiss, granite, gneiss	3	88.30
Transvaal	dolomite	9	0.27

Source: own study.

Hydraulic conductivity (*C*). *C* is defined as the capability of an aquifer formation to transmit water via pore spaces or fractures when subjected to the hydraulic gradient [KHOSRAVI *et al.* 2018]. It determines the rate of contaminant travel, residence time and attenuation potential. However, it depends on properties of water (especially its kinematic viscosity and density) and aquifer (rock material) [SINGHAL, GUPTA 2010; YOUNGER 2009]. Well sorted and coarse-grained materials will have a higher hydraulic conductivity than fined grained materials, such as silt and clay. Compaction and intrusion of impermeable layers (cementation) due to various construction activities can significantly reduce the *C*. This could be demonstrated more in urban areas due to the anthropogenic activity (for example, deep excavations for constructions of multi-storey buildings, subsurface pipes, etc.). In hard fractured rocks, such as genesis, granites *etc*., the hydraulic conductivity depends on size, density and interconnection of fractures [SINGHAL, GUPTA 2010]. On the one hand, rocks with higher conductivity permit water and contaminants to move and spread quickly into groundwater, resulting in increased groundwater vulnerability (*GWV*). On the other hand, rocks with low *C* values restrict water and contaminant movement, eventually making groundwater less vulnerable to pollution.

The measured values for the *C* were not available in the study area. Hence, the approximate hydraulic conductivity values for various rocks were extracted from hydrogeological literature, such as DOMENICO and SCHWARTZ [1998] and YOUNGER [2009]. These values were further divided into seven classes (Fig. 10, Tab. 10). The values have been rated, and the higher rating is given to higher conductivity, while lower ratings to lower conductivity. The *C* of the dolomitic aquifer is assigned to the highest rating (10), since such aquifers have high permeability due to their karstic formations [OUEDRAOGO *et al.* 2016]. These aquifers cover a tiny portion of the area and they are located in the north end of the sub-catchment. The Witwatersrand lithological formation was given a rating of 6, whereas the Vetersdrop formation was rated 4. The lowest rating (3) was assigned to granite-

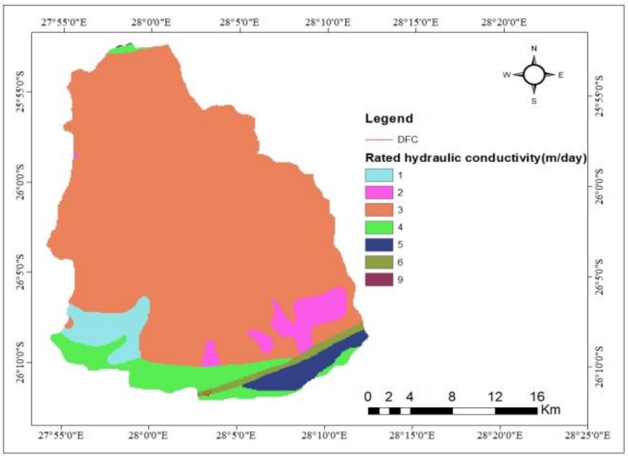

Fig. 10. Rated map of hydraulic conductivity (*C*); source: own study

Table 10. Rates and coverage of hydraulic conductivity

Lithology description	Range ($m \cdot day^{-1}$)	Rate	Area (%)
Dolomite	10^3–10^2	9	0.02
Lava (mainly andesite and quartzite, porphyry), shale and quartzite	10^{-4}–10^{-2}	5	2.73
Amphibolite, serpentinite, talc, schist, diorite, gabbro, pyroxenite	10^{-5}–10^{-4}	2	4.01
Dunite	10^{-6}–10^{-5}	1	3.98
Genesis, magmatic and granite	10^{-5}–10^{-3}	3	80.33
Quartzites, shales and conglomerates	10^{-5}–10^{-2}	4	7.42
Tholeiitic basalt (andesite, tuff)	10^{-4}–10^{-1}	6	1.49

Source: own study.

genes, which cover most of the Quaternary catchment area. The weighting of 3 was assigned to the *C*, according to ALLER *et al.* [1987] and LYNCH *et al.* [1994] recommendations.

GROUNDWATER VULNERABILITY

RASTIC INDEX

DRASTIC index values were divided into four classes using natural breaks (Jenks) classification techniques and the results are shown in Figure 11 and Table 11. The *GWV* index ranged from 80 to 162, where higher values indicate the potentials of hydrogeological and landscape parameters to readily move contaminants to groundwater, while a low value shows that resource has better protection from pollutants. The results reveal that about 6.6% (48.93 km^2) of the area, mostly in the southern side of the sub-catchment, has very high vulnerability. About 53.6% (408 km^2) of the

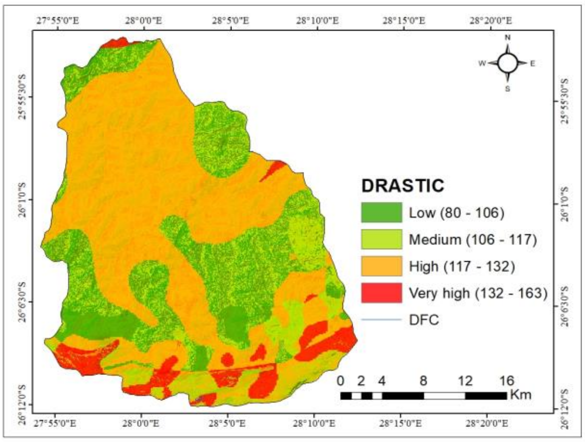

Fig. 11. Vulnerability index map using DRASTIC model; source: own study

Table 11. Results of vulnerability classes

Index range	Vulnerability class	DRASTIC model coverage	
		area (km^2)	area (%)
80–106	low	165.13	21.7
106–117	medium	137.52	18.1
117–132	high	408.00	53.6
132–163	very high	49.93	6.6
Total		**760.58**	**100**

Source: own study.

catchments area also exhibited high risk of groundwater contamination. It is located mostly in central, north-eastern and western parts of the sub-catchment. Medium and low vulnerability classes cover only 18.1% (137.5 km^2) and 21.7% (165.1 km^2) of the study area, respectively. According to Figure 11, the shallow groundwater of the DFC campus can be classified as highly vulnerable.

The southern part, where the DFC campus is located, central, north-eastern and western parts of the area are mostly fall into the category of very high vulnerability. The possible reason for this could be high urbanisation in the southern side and agricultural area in the north part of the catchment. The study area is drained by the Jukskei River which starts from the southern border of the area (around the Doorfountien campus) and with its tributaries drains to the north. The Jukskei River catchment is one of catchments having a serious contamination problem [HUIZENGA, HARMSE 2005]. Water quality problems are mainly caused by geological and anthropogenic factors, such as increased communal effluent discharge due to high urbanisation and industrial activities [HUIZENGA, HARMSE 2005]. Uncontrolled release of effluents in the urban area usually elevates the NO_3 concentration and increases groundwater vulnerability.

THE SENSITIVITY OF DRASTIC MODEL PARAMETERS

The statistical summary of hydrogeological factors applied to develop the DRASTIC model are shown in Table 12. The *R* and *A* parameters show higher mean values of 7.0 and 7.4, respectively, whereas the *C* parameters have the lowest mean rate (4.28). All other parameters' mean rates range from 5.25 to 5.88. The highest coefficient of variation (*CV* = 66.47) is observed regarding the *D* parameter followed by *T* (*CV* = 61.42) and *C* (*CV* = 58.17) parameters, whereas the lowest variation (*CV* = 9.09) is observed for the *S* parameter. Other parameters exhibited moderate variations. Higher *CV* values of DRASTIC parameters suggest a significant contribution of such parameters to the variation in GV, whereas parameters with lower *CV* values indicate less contribution to the variation of GV [BABIKER *et al.* 2005; VU *et al.* 2019].

Single parameter sensitivity analysis. The results of single parameter sensitivity analysis computed by Equation (2) for DRASTIC are shown in Table 13. According to the

Table 12. Statistical summary of DRASTIC parameters

Parameter	Minimum	Maximum	Mean	Standard deviation	Coefficient of variation (*CV*%)
D	1	10	5.25	3.49	66.47
R	6	8	7.00	1.00	14.28
A	4	10	7.40	2.15	29.05
S	5	6	5.50	0.50	9.09
T	1	10	5.60	3.44	61.42
I	3	9	5.50	2.29	41.63
C	1	9	4.28	2.49	58.17

Explanations: *D* = depth to water level, *R* = net recharge, *A* = aquifer media, *S* = soil media, *T* = topography, *I* = impact of the vadose zone, and *C* = the hydraulic conductivity.
Source: own study.

table, the effective weight of some parameters is higher, whereas others show deviation from their respective theoretical weights assigned. The depth to water level (*D*) has higher effective weight (22.4%) which exceeds its theoretical weight. It indicated that *D* is the most significant parameter for vulnerability assessment. The net recharge, aquifer media, soil and topography also show higher effective weights (20.49, 19.93, 10.21 and 5.3%) and higher effective weights (20.49, 19.93, 10.21 and 5.3%) compared to their theoretical weights (17.39, 13.04, 8.69 and 4.34%), respectively. However, the impact of vadose zone and hydraulic conductivity has lower effective weights (13.87 and 7.75%) than theoretically assigned weights (21.73 and 13.04%), respectively.

Table 13. Statistical summary of single parameter sensitivity analysis

Parameter	Theoretical weight	Theoretical weight (%)	Effective weight (%)			
			minimum	maximum	mean	*SD*
D	5	21.73	5.05	40.98	22.40	7.36
R	4	17.39	14.81	29.27	20.49	2.05
A	3	13.04	9.30	28.57	19.93	3.00
S	2	8.69	6.41	14.63	10.21	1.04
T	1	4.34	0.68	10.75	5.30	2.02
I	5	21.73	10.42	33.33	13.87	3.25
C	3	13.04	2.44	16.67	7.75	1.74

Explanations as in Tab. 12.
Source: own study.

Map removal sensitivity analysis. The analysis of map removal sensitivity is indicated in Table 14. Results show variability when a single parameter is removed from the vulnerability index at a time. The *T* parameter has a relatively high mean map removal sensitivity variation index (1.49%) – Table 14, despite its low theoretical and effective weights (Tab. 13). The vulnerability index has also shown sensitivity when the *D* parameter is removed from the vulnerability analysis (mean variation index of 1.44%). The vulnerability index is much less sensitive to the *I* factor and moderately sensitive to *A*, *R*, *S* and *C*.

Table 14. Statistical summary of map removal sensitivity analysis

Parameter removed	Variation index (%)			
	minimum	maximum	mean	*SD*
D	0	4.45	1.44	1.12
R	0.08	2.49	1.03	0.34
A	0.02	2.38	0.98	0.40
S	0	1.31	0.68	0.17
T	0.59	2.26	1.49	0.33
I	0	3.17	0.36	0.04
C	0	1.97	1.08	0.28

Explanations as in Tab. 12.
Source: own study.

VALIDATION OF VULNERABILITY INDEX MAPS

The NO_3^- values superimposed on the vulnerability index map is shown in Figure 12. In the map, maximum NO_3^- values coincide with areas characterised by high and very high groundwater vulnerability zones. The scatter plot of

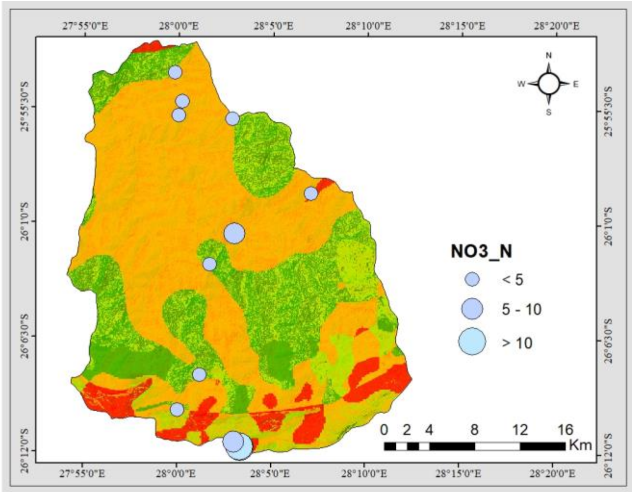

Fig. 12. Spatial distribution of nitrate on the DRASTIC vulnerability index map; source: own study

nitrate concentrations versus DRASTIC index values are also shown in Figure 13. The line of the best fit in plots shows a moderate positive correlation (R^2 = 0.5) between the DRASTIC and nitrate concertation demonstrating the agreement between the computed vulnerability and risks of pollution (Fig. 13). The validation shows the applicability of the model to the urbanised environment.

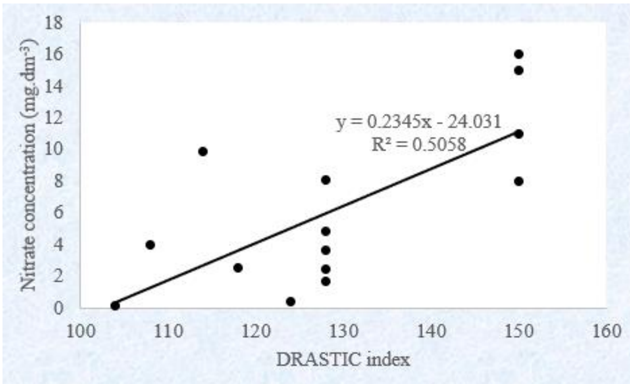

Fig. 13. Plot of nitrate concentration versus DRASTIC index

CONCLUSIONS

This study assessed vulnerability of groundwater to contamination in urbanised and hard rock environments by using the DRASTIC model. Seven natural hydrogeological parameters were considered for the model. The results reveal that about 6.6% (48.93 km^2) of the area, mostly in the southern side of the sub-catchment, has very high vulnerability. About 53.6% (408 km^2) of the catchment area also exhibited high risk of groundwater contamination and it is located mostly in central, north-eastern and western parts of the sub-catchment. The medium and low vulnerability cover only 18.1% (137.5 km^2) and 21.7% (165.1 km^2) of the study area, respectively. The shallow groundwater at the DFC campus is a part of a very high vulnerability area. Sensitivity analyses performed to determine the effect of parameters on the vulnerability index indicate that *D*, *R*, *A*, *S* and *T* are important contributors to the vulnerability assessment using the DRASTIC model. The analysis of nitrate and DRASTIC models show a positive moderate correlation. It indicates that the resources are less protected against surface contamination. Thus, protective measures should be put in place to protect the groundwater reserve from surface pollutants originating from natural and anthropogenic activities. The result of this study helps to provide qualitative information for groundwater monitoring and can further be improved and verified by using other vulnerability assessment models.

ACKNOWLEDGEMENTS

The first author acknowledges the University of Johannesburg for offering the Global Excellence and Stature (GES) scholarship for the doctoral study. The Department of Water and Sanitation and the South African Council for Geoscience are also acknowledged for providing data.

REFERENCES

ABIYE T.A. 2011. Provenance of groundwater in the crystalline aquifer of Johannesburg area, South Africa. International Journal of Physical Sciences. Vol. 6. Iss. 4 p. 98–111. DOI 10.5897/IJPS10.119.

ABIYE T.A., MENGISTU H., DEMLIE M.B. 2011. Groundwater resource in the crystalline rocks of the Johannesburg area, South Africa. Journal of Water Resources and Protection. Vol. 3 p. 199–212. DOI 10.4236/jwarp.2011.34026.

AKBAR T.A., AKBAR R.A. 2013. Pesticide health risk mapping and sensitivity analysis of parameters in groundwater vulnerability assessment. Clean Soil Air Water. Vol. 41. Iss. 11 p. 1073–1079. DOI 10.1002/clen.201200232.

ALLER L., BENNETT T., LEHR J.H., PETTY R.J., HACKETT G. 1987. DRASTIC: A standardized system for evaluating groundwater pollution potential using hydrogeologic settings. U.S. Environmental Protection Agency. Washington. D.C., EPA/600/2-85/018. pp. 163.

AYDI A. 2018. Evaluation of groundwater vulnerability to pollution using a GIS-based multi-criteria decision analysis. Groundwater for Sustainable Development. Vol. 7 p. 204–211. DOI 10.1016/j.gsd.2018.06.003.

BABIKER I.S., MOHAMED M.A., HIYAMA T., KATO K. 2005. A GIS-based DRASTIC model for assessing aquifer vulnerability in Kakamigahara Heights, Gifu Prefecture, central Japan. Science of The Total Environment. Vol. 345. Iss. 1–3 p. 127–40. DOI 10.1016/j.scitotenv.2004.11.005.

BARNARD H.C. 1999. Hydrogeological map of Johannesburg 2526. 1:500.000. Department of Water Affairs and Forestry, Pretoria, Johannesburg, RSA.

BOUFEKANE A., SAIGHI O. 2018. Application of groundwater vulnerability overlay and index methods to the Jijel Plain Area (Algeria). Ground Water. Vol. 56. Iss. 1 p. 143–156. DOI 10.1111/gwat.12582.

BUTLER A.P.2010. Groundwater vulnerability and protection. In: Groundwater modelling in arid and semi-arid areas. Eds. H.S. Wheater, S.A. Mathias, X. Li. International Hydrology Series. Cambridge. Cambridge University Press p. 75–86. DOI 10.1017/CBO9780511760280.007.

CHEN J., WU H., QIAN H., LI X. 2018. Challenges and prospects of sustainable groundwater management in an agricultural plain along the Silk Road Economic Belt, north-west China. International Journal of Water Resources Development. Vol. 34. Iss. 3 p. 354–368. DOI 10.1080/07900627.2016.1238348.

DE BEER J.H. 1986. Geology of Johannesburg, Republic of South Africa. Environmental and Engineering Geoscience. Vol. 23. Iss. 2 p. 101–137. DOI 10.2113/gseegeosci.xxiii.2.101.

DEVIC G., DJORDJEVIC D., SAKAN S. 2014. Natural and anthropogenic factors affecting the groundwater quality in Serbia. Science of the Total Environment. Vol. 468-469 p. 933–941. DOI 10.1016/j.scitotenv.2013.09.011.

DOMENICO P.A., SCHWARTZ F.W. 1997. Physical and chemical hydrogeology. 2nd ed. Wiley New York. ISBN 978-0-471-59762-9 pp. 528.

DWAF 2006. Groundwater Resource Assessment II: Task 3aE Recharge, final report. Department of Water Affairs and Forestry. Pretoria, South Africa pp. 129.

DWS 2019. National Integrated Water Information System (NIWIS) [on-line]. Department of Water and Sanitation, Republic of South Africa. [Access 18.12.2019]. Available at: http://www.dwa.gov.za/niwis2/GroundWaterStatus.

GUPTA N. 2014. Groundwater vulnerability assessment using DRASTIC method in Jabalpur District of Madhya Pradesh. International Journal of Recent Technology and Engineering. Vol. 3. Iss. 3 p. 36–43.

HAMUTOKO J.T., WANKE H., VOIGT H.J. 2016. Estimation of groundwater vulnerability to pollution based on DRASTIC in the Niipele sub-basin of the Cuvelai Etosha Basin, Namibia. Physics and Chemistry of the Earth. Parts A/B/C. Vol. 93 p. 46–54. DOI 10.1016/j.pce.2015.12.007.

HASAN M., ISLAM M.A., AZIZ HASAN M., ALAM M.J., PEAS M.H. 2019. Groundwater vulnerability assessment in Savar upazila of Dhaka district, Bangladesh – A GIS-based DRASTIC modeling. Groundwater for Sustainable Development. Vol. 9, 100220. DOI 10.1016/j.gsd.2019.100220.

HOWARD K.W.F. 2014. Sustainable cities and the groundwater governance challenge. Environmental Earth Sciences. Vol. 73. Iss. 6 p. 2543–2554. DOI 10.1007/s12665-014-3370-y.

HUANG L., ZENG G., LIANG J., HUA S., YUAN Y., LI X., DONG H., LIU J., NIE S., LIU J. 2017. Combined impacts of land use and climate change in the modeling of future groundwater vulnerability. Journal of Hydrologic Engineering. Vol. 22. Iss. 7, 05017007. DOI 10.1061/(ASCE)HE.1943-5584.0001493.

HUIZENGA J.M., HARMSE J.T. 2005. Geological and anthropogenic influences on the inorganic water chemistry of the Jukskei River, Gauteng, South Africa. South African Journal of Geology. Vol. 108. Iss. 3 p. 439–447. DOI 10.2113/108.3.439.

JAHAN C.S., RAHAMAN M.F., AREFIN R., ALI M.S., MAZUMDER Q.H. 2018. Delineation of groundwater potential zones of Atrai–Sib River basin in north-west Bangladesh using remote sensing and GIS techniques. Sustainable Water Resources Management. Vol. 5. Iss. 3 p. 689–702. DOI 10.1007/s40899-018-0240-x.

JANG W.S., ENGEL B., HARBOR J., THELLER L. 2017. Aquifer vulnerability assessment for sustainable groundwater management using DRASTIC. Water. Vol. 9. Iss. 10 p. 792–792. DOI 10.3390/w9100792.

KADAOUI M., BOUALI A., ARABI M. 2019. Assessment of physico-chemical and bacteriological groundwater quality in irrigated Triffa Plain, North-East of Morocco. Journal of Water and Land Development. No. 42 (VII–IX) p. 100–109. DOI 10.2478/jwld-2019-0050.

KHOSRAVI K., SARTAJ M., TSAI F.T., SINGH V.P., KAZAKIS N., MELESSE A.M., PRAKASH I., TIEN BUI D., PHAM B.T. 2018. A comparison study of DRASTIC methods with various objective methods for groundwater vulnerability assessment. Science of The Total Environment. Vol. 642 p. 1032–1049. DOI 10.1016/j.scitotenv.2018.06.130.

KIHUMBA A.M., VANCLOOSTER M., LONGO J.N. 2017. Assessing groundwater vulnerability in the Kinshasa region, DR Congo, using a calibrated DRASTIC model. Journal of African Earth Sciences. Vol. 126 p. 13–22. DOI 10.1016/j.jafrearsci.2016.11.025.

KOSITCIN N., MCNAUGHTON N.J., GRIFFIN B.J., FLETCHER I.R., GROVES D.I., RASMUSSEN B. 2003. Textural and geochemical discrimination between xenotime of different origin in the Archaean Witwatersrand Basin, South Africa. Geochimica et Cosmochimica Acta. Vol. 67. Iss. 4 p. 709–731. DOI 10.1016/S0016-7037(02)01169-9.

KOZŁOWSKI M., SOJKA M. 2019. Applying a modified DRASTIC model to assess groundwater vulnerability to pollution: A case study in Central Poland. Polish Journal of Environmental Studies. Vol. 28. Iss. 3 p. 1223–1231. DOI 10.15244/pjoes/84772.

KUMAR A., KRISHNA A.P. 2019. Groundwater vulnerability and contamination risk assessment using GIS-based modified DRASTIC-LU model in hard rock aquifer system in India. Geocarto International. Vol. 35. Iss. 11 p. 1149–1178. DOI 10.1080/10106049.2018.1557259.

LODWICK W.A., MONSON W., SVOBODA L. 1990. Attribute error and sensitivity analysis of map operations in geographical information systems: Suitability analysis. International Journal of Geographical Information Systems. Vol. 4. Iss. 4 p. 413–428. DOI 10.1080/02693799008941556.

LYNCH S.D., REYNDERS A.G., SCHULZE R.E. 1994. Preparing input data for a national-scale groundwater vulnerability map of southern Africa. Water SA. Vol. 20. Iss. 3 p. 239–246.

LYNCH S.D., REYNDERS A.G., SCHULZE, R.E. 1997. A DRASTIC approach to groundwater vulnerability in South Africa. South African Journal of Science (South Africa). Vol. 93. Iss. 2 p. 59–60.

MACHIWAL D., CLOUTIER V., GÜLER C., KAZAKIS N. 2018a. A review of GIS-integrated statistical techniques for groundwater quality evaluation and protection. Environmental Earth Sciences. Vol. 77. Iss. 19, 681. DOI 10.1007/s12665-018-7872-x.

MACHIWAL D., JHA M.K., SINGH V.P., MOHAN C. 2018b. Assessment and mapping of groundwater vulnerability to pollution: Current status and challenges. Earth-Science Reviews. Vol. 185 p. 901–927. DOI 10.1016/j.earscirev.2018.08.009.

MALHERBE H., GEBEL M., PAULEIT S., LORZ C. 2018. Land use pollution potential of water sources along the southern coast of South Africa. Change and Adaptation in Socio-Ecological Systems. Vol. 4. Iss. 1 p. 7–20. DOI 10.1515/cass-2018-0002.

MCCARTHY T., RUBIDGE B. 2005. The story of earth & life: A South African perspective on a 4,6-billion-year journey. Cape Town. Struik Publishers. ISBN 978-1770071483 pp. 333.

MUHAMMAD A.M., ZHONGHUA T., DAWOOD A.S., EARL B. 2015. Evaluation of local groundwater vulnerability based on DRASTIC index method in Lahore, Pakistan. Geofísica Internacional. Vol. 54. Iss. 1 p. 67–81. DOI 10.1016/ j.gi.2015.04.003.

MUSEKIWA C., MAJOLA K. 2013. Groundwater vulnerability map for South Africa. South African Journal of Geomatics. Vol. 2. Iss. 2 p. 152–162.

NAPOLITANO P., FABBRI A.G. 1996. Single-parameter sensitivity analysis for aquifer vulnerability assessment using DRASTIC and SINTACS. HydroGIS 96: Application of Geographic Information Systems in Hydrology and Water Resources Management (Proceedings of the Vienna Conference, April 1996). IAHS Publication. No. 235 p. 559–566.

National Research Council 1993. Ground water vulnerability assessment: Predicting relative contamination potential under conditions of uncertainty. Washington, DC. The National Academies Press. ISBN 978-0-309-04799-9 pp. 224. DOI 10.17226/2050.

NESHAT A., PRADHAN B., DADRAS M. 2014. Groundwater vulnerability assessment using an improved DRASTIC method in GIS. Resources, Conservation and Recycling. Vol. 86 p. 74–86. DOI 10.1016/j.resconrec.2014.02.008.

OKE S.A., FOURIE F. 2017. Guidelines to groundwater vulnerability mapping for Sub-Saharan Africa. Groundwater for Sustainable Development. Vol. 5 p. 168–177. DOI 10.1016/j.gsd.2017.06.007.

OUEDRAOGO I., DEFOURNY P., VANCLOOSTER M. 2016. Mapping the groundwater vulnerability for pollution at the pan African scale. Science of The Total Environment. Vol. 544 p. 939–953. DOI 10.1016/j.scitotenv.2015.11.135.

RIBEIRO L., PINDO J.C., DOMINGUEZ-GRANDA L. 2017. Assessment of groundwater vulnerability in the Daule aquifer, Ecuador, using the susceptibility index method. Science of The Total Environment. Vol. 574 p. 1674–1683. DOI 10.1016/j.scitotenv.2016.09.004.

SAAYMAN I., BEEKMAN H., ADAMS S., CAMPBELL R., CONRAD J., FEY M., JOVANOVIC N., THOMAS A., USHER B. 2007. Assessment of aquifer vulnerability in South Africa. Report to the Water Research Commission: WRC Report No. 1432/1/07. Pretoria, South Africa.

SAIDI S., BOURI S., BEN DHIA H. 2011. Sensitivity analysis in groundwater vulnerability assessment based on GIS in the Mahdia-Ksour Essaf aquifer, Tunisia: a validation study. Hydrological Sciences Journal. Vol. 56. Iss. 2 p. 288–304. DOI 10.1080/02626667.2011.552886.

SAKALA E., FOURIE F., GOMO M., COETZEE H. 2018. GIS-based groundwater vulnerability modelling: A case study of the Witbank, Ermelo and Highveld Coalfields in South Africa. Journal of African Earth Sciences. Vol. 137 p. 46–60. DOI 10.1016/j.jafrearsci.2017.09.012.

SHRESTHA S., KAFLE R., PANDEY V.P. 2017. Evaluation of index-overlay methods for groundwater vulnerability and risk assessment in Kathmandu Valley, Nepal. Science of The Total Environment. Vol. 575 p. 779–790. DOI 10.1016/j.scitotenv.2016.09.141.

SINGH A., SRIVASTAV S.K., KUMAR S., CHAKRAPANI G.J. 2015. A modified-DRASTIC model (DRASTICA) for assessment of groundwater vulnerability to pollution in an urbanized environment in Lucknow, India. Environmental Earth Sciences. Vol. 74. Iss. 7 p. 5475–5490. DOI 10.1007/s12665-015-4558-5.

SINGHAL B.B.S., GUPTA R.P. 2010. Applied hydrogeology of fractured rocks. 2nd ed. Springer Science and Business Media. ISBN 978-94-007-9019-3 pp. 408.

VU T.-D., NI C.-F., LI W.-C., TRUONG M.-H.J.W. 2019. Modified index-overlay method to assess spatial–temporal variations of groundwater vulnerability and groundwater contamination risk in areas with variable activities of agriculture developments. Water. Vol. 11. Iss. 12, 2492. DOI 10.3390/w11122492.

Water resources of South Africa, 2012 Study (WR2012) [online]. [Access 29.09.2019]. Available at: http://waterresourceswr2012.co.za

YOUNGER P.L. 2009. Groundwater in the environment: An introduction. London. John Wiley & Sons. ISBN 9781444309041 pp. 336.